

Short Course on Experimental Dynamic Substructuring

Module #8: Geometrically nonlinear systems



Matthew S. Allen

Professor, Engineering Physics Dept, University of Wisconsin-Madison

Randall L. Mayes

Distinguished Member of Technical Staff, Sandia National Labs.

Paolo Tiso

Senior Scientist, Dept. of Mechanical and Process Eng., ETH Zürich

Short Course Notes For:

February 8, 2020, IMAC, Houston, TX, USA

1

Outline

- **Geometric nonlinearities**
 - Bending-stretching coupling
 - Von-Karman beam/plate equation
 - Vibration modes for reduction?
- **Modal derivatives**
 - Definition
 - Dynamic modal derivatives
 - Static modal derivatives
- **Hurty-Craig-Bampton for geometric nonlinearities**
 - interface reduction
 - Modal derivatives of internal and interface modes
- **Flexible multibody systems**
 - Floating frame of reference
 - HCB vs Rubin
- **Summary**

2

Geometric Nonlinearities



Definition: geometrical nonlinearities are into play if the **change of geometry** of the system **under loading** cannot be neglected because **it influences the loading** (in amplitude and direction)

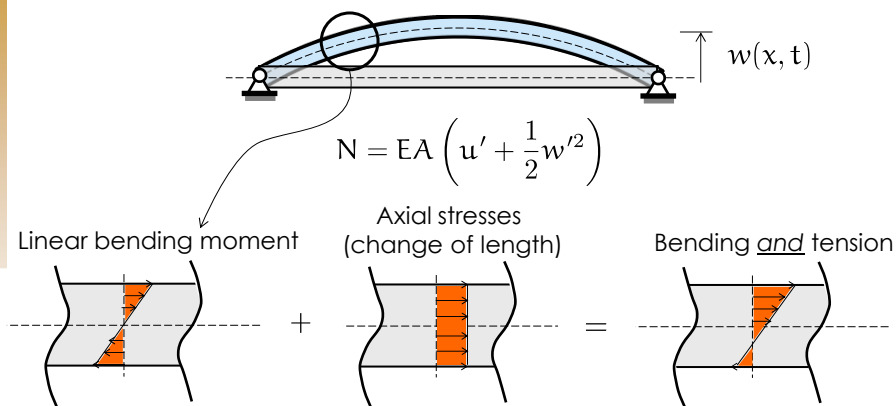
	Linear	Nonlinear
Displacements	Small	Large
Rotations	Small	Large
Strains	Small	Small/large

- ✓ *Multibody systems*
- ✓ *Thin-walled structures*

Short Course on Experimental Dynamic Substructuring, © 2020

3

String Effect



Bending-stretching coupling

O. Thomas, A. S  n  chal, J.-F. De  , **Hardening/softening behavior and reduced order modeling of nonlinear vibrations of rotating cantilever beams**, *Nonlinear Dynamics*, 2016.

Short Course on Experimental Dynamic Substructuring,    2020

Short Course on Experimental Dynamic Substructuring,    2020

11-2-2020#

4

von Karman beam FE equation

In/out of plane coupling via nonlinear terms:

$$\begin{bmatrix} \mathbf{M}_{ww} & \mathbf{0} \\ \mathbf{0} & \mathbf{M}_{uu} \end{bmatrix} \begin{bmatrix} \ddot{\mathbf{w}} \\ \ddot{\mathbf{u}} \end{bmatrix} + \begin{bmatrix} \mathbf{K}_{ww} & \mathbf{0} \\ \mathbf{0} & \mathbf{K}_{uu} \end{bmatrix} \begin{bmatrix} \mathbf{w} \\ \mathbf{u} \end{bmatrix} + \begin{bmatrix} {}_2\mathbf{f}_w(\mathbf{w}, \mathbf{u}) \\ {}_2\mathbf{f}_u(\mathbf{w}, \mathbf{w}) \end{bmatrix} + \begin{bmatrix} {}_3\mathbf{f}_w(\mathbf{w}, \mathbf{w}, \mathbf{w}) \\ \mathbf{0} \end{bmatrix} = \begin{bmatrix} \mathbf{q}_w \\ \mathbf{0} \end{bmatrix}$$

- Linearly decoupled (beam and bar)
- This particular structure of the nonlinear terms only due to the symmetry of the system
- For thin-walled structures, still one can distinguish between **slow, bending** dominated dynamics and **fast, axial** dominated dynamics; this is a key ingredient for model order reduction

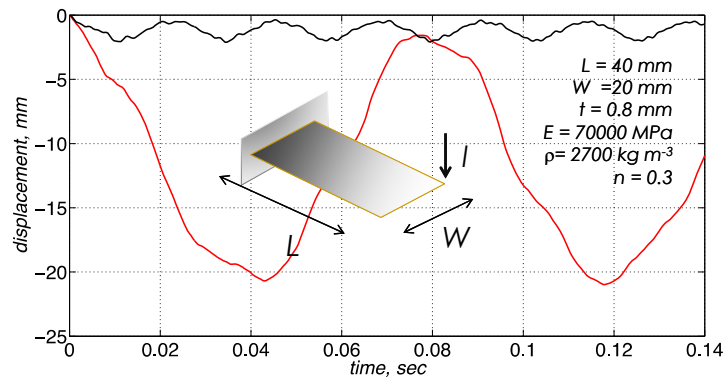
Short Course on Experimental Dynamic Substructuring, © 2020

5

5

Vibration modes?

$$[\mathbf{K} - \omega_i^2 \mathbf{M}] \boldsymbol{\phi}_i = \mathbf{0} \quad \boldsymbol{\Phi} = [\boldsymbol{\phi}_1, \dots, \boldsymbol{\phi}_m]$$



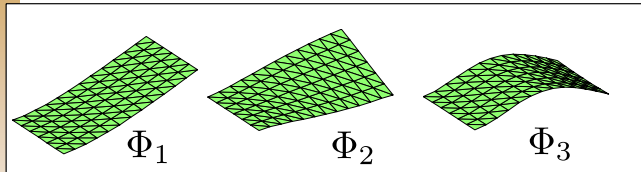
P. Tiso, *Optimal second order reduction basis selection for nonlinear transient analysis*, IMAC-XXIX, 2011.

Short Course on Experimental Dynamic Substructuring, © 2020

6

What is missing?

Slow vibration modes only contain out-of-plane displacements:



$$\Phi = \begin{bmatrix} \Phi_w \\ \Phi_u \end{bmatrix} = \begin{bmatrix} \Phi_w \\ 0_u \end{bmatrix}$$

Overly-stiff behavior!

$$\begin{bmatrix} \mathbf{M}_{ww} & \mathbf{0} \\ \mathbf{0} & \mathbf{M}_{uu} \end{bmatrix} \begin{bmatrix} \ddot{\mathbf{w}} \\ \ddot{\mathbf{u}} \end{bmatrix} + \begin{bmatrix} \mathbf{K}_{ww} & \mathbf{0} \\ \mathbf{0} & \mathbf{K}_{uu} \end{bmatrix} \begin{bmatrix} \mathbf{w} \\ \mathbf{u} \end{bmatrix} + \begin{bmatrix} {}_2\mathbf{f}_w(\mathbf{w}, \mathbf{u}) \\ {}_2\mathbf{f}_u(\mathbf{w}, \mathbf{w}) \end{bmatrix} + \begin{bmatrix} {}_3\mathbf{f}_w(\mathbf{w}, \mathbf{w}, \mathbf{w}) \\ \mathbf{0} \end{bmatrix} = \begin{bmatrix} \mathbf{q}_w \\ \mathbf{0} \end{bmatrix}$$

Need appropriate in-plane contributions. Seeking them between the set of high-frequency eigenmodes is not a good option:

1. Which ones?
2. Need to extract a lot of them. For large systems, this is expensive.

Short Course on Experimental Dynamic Substructuring, © 2020

7

Modal Derivatives - definition

For geometrically nonlinear structural dynamics, slow vibration modes are still the dominant ingredient of the response

$$(\mathbf{K}|_{eq} - \omega_i^2 \mathbf{M}) \phi_i = \mathbf{0} \quad \mathbf{u}(t) \approx \sum_{i=1}^m \phi_i \eta_i(t) = \Phi \mathbf{q}(t),$$

Then, we need to know how modes change under underlying finite displacements.

$$(\mathbf{K}|_{eq} - \omega_i^2|_{eq} \mathbf{M}) \frac{\partial \phi_i}{\partial q_j} \Big|_{eq} + \left(\frac{\partial \mathbf{K}}{\partial q_j} \Big|_{eq} - \frac{\partial \omega_i^2}{\partial q_j} \Big|_{eq} \mathbf{M} \right) \phi_i|_{eq} = \mathbf{0}$$

Modal derivative

The *directional derivative* of the stiffness matrix is defined as

$$\frac{\partial \mathbf{K}}{\partial q_j} \Big|_{eq} = \frac{\partial \mathbf{K}(\mathbf{u} = \eta_j \phi_j|_{eq})}{\partial q_j} \Big|_{q_j=0}$$

Short Course on Experimental Dynamic Substructuring, © 2020

8

Modal derivatives - calculation

Recall the orthogonality property of vibration modes

$$\phi_i^T \mathbf{M} \phi_i = 1 \quad \forall i \in \{1, 2, \dots, m\}.$$

Differentiating and accounting for symmetry of \mathbf{M}

$$\phi_i^T \mathbf{M} \frac{\partial \phi_i}{\partial q_j} + \phi_i^T \mathbf{M}^T \frac{\partial \phi_i}{\partial q_j} = 0 \quad \forall i, j \in \{1, 2, \dots, m\}$$

$$\phi_i^T|_{eq} \mathbf{M} \frac{\partial \phi_i}{\partial q_j} \Big|_{eq} = 0 \quad \forall i, j \in \{1, 2, \dots, m\}$$

This gives an extra condition to close the system: direct method

$$\begin{bmatrix} [\mathbf{K}|_{eq} - \omega_i^2|_{eq} \mathbf{M}]_{n \times n} & -[\mathbf{M} \phi_i|_{eq}]_{n \times 1} \\ -[\mathbf{M} \phi_i|_{eq}]_{1 \times n}^T & 0_{1 \times 1} \end{bmatrix} \begin{bmatrix} [1] \frac{\partial \phi_i}{\partial q_j} \Big|_{eq} \\ \frac{\partial \omega_i^2}{\partial q_j} \Big|_{eq} \end{bmatrix} = \begin{bmatrix} -\frac{\partial \mathbf{K}}{\partial q_j} \Big|_{eq} \phi_i|_{eq} \\ 0 \end{bmatrix}.$$

Short Course on Experimental Dynamic Substructuring, © 2020

9

Static Modal Derivatives

Problem with the definition: it is questionable if *modal amplitudes* (i.e. structural displacements) can be treated as *parameters*. Does sensitivity make sense?

It was early proposed [1] to “*neglect the mass matrix*”, which leads to the *Static Modal Derivatives* (SMDs)

$$\mathbf{K}|_{eq} \frac{\partial \phi_i}{\partial q_j} \Big|_{eq}^s = - \frac{\partial \mathbf{K}}{\partial q_j} \Big|_{eq} \phi_i|_{eq}$$

Bring a lot of advantages:

- ✓ Easier to compute: set of linear problems with same \mathbf{K}
- ✓ More consistent with the physics (more on this later)
- ✓ Symmetric ($m^*(m+1)/2$ SMDs)

$$\frac{\partial \phi_i}{\partial q_j} \Big|_{eq}^s = \frac{\partial \phi_j}{\partial q_i} \Big|_{eq}^s$$

[1] Idelsohn, S. R., Cardona, A. *A reduction method for nonlinear structural dynamic analysis*, CMAME (1985)

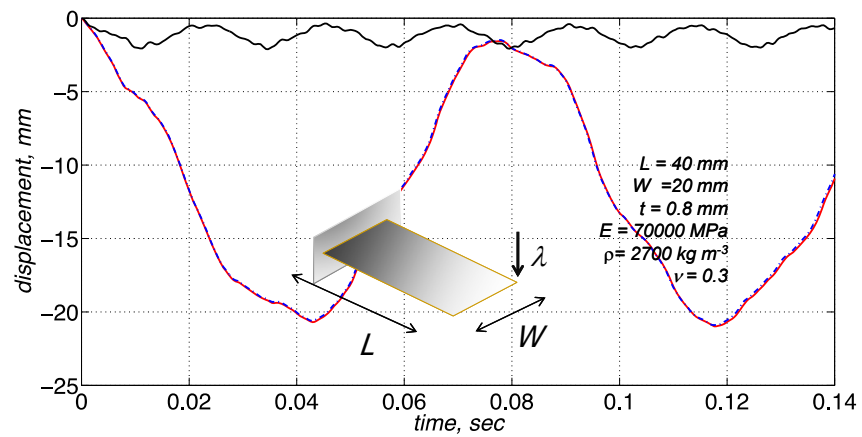
Short Course on Experimental Dynamic Substructuring, © 2020

10

Modal Derivatives - effectiveness

$$\Phi = [\phi_1, \dots, \phi_m, \dots, \theta_{ij}, \dots]$$

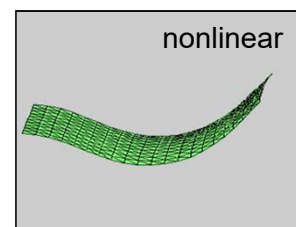
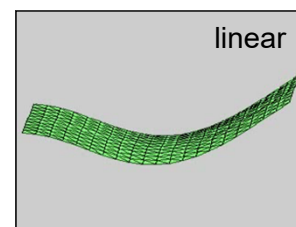
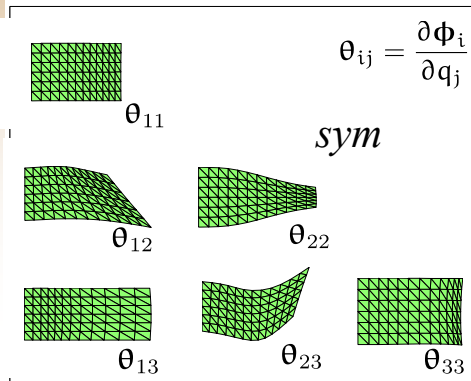
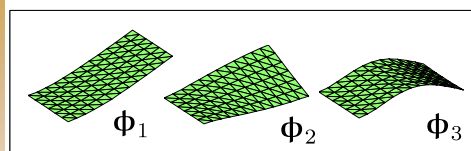
Basis enrichment



Short Course on Experimental Dynamic Substructuring, © 2020

11

Physical Interpretation



Short Course on Experimental Dynamic Substructuring, © 2020

12

Motivation

- Several systems are characterized by components that might undergo nonlinear deformations
- Nonlinear elastic behavior might be superimposed to rigid body motion
- It is convenient to analyze the components alone as much as possible

Based on:

L. Wu, P. Tiso, *A Modal Derivatives Enhanced Craig-Bampton Method for Geometrically Nonlinear Structures*, preprint

13

13

Possible Applications



Short Course on Experimental Dynamic Substructuring, © 2020

14

Theory

Each substructure is assumed geometrically nonlinear

$$\mathbf{M}_{(s)} \ddot{\mathbf{u}}_{(s)}\{t\} + \mathbf{f}_{(s)}\{\mathbf{u}_{(s)}\{t\}\} = \mathbf{g}_{(s)}\{t\} + \mathbf{p}_{(s)}\{t\}, \quad s = 1, \dots, H$$

Linearize:

$$\begin{bmatrix} \mathbf{M}_{(s)}^{BB} & \mathbf{M}_{(s)}^{BI} \\ \mathbf{M}_{(s)}^{IB} & \mathbf{M}_{(s)}^{II} \end{bmatrix} \begin{bmatrix} \ddot{\mathbf{q}}_{(s)}^B \\ \ddot{\mathbf{q}}_{(s)}^I \end{bmatrix} + \begin{bmatrix} \bar{\mathbf{K}}_{(s)}^{BB} & \bar{\mathbf{K}}_{(s)}^{BI} \\ \bar{\mathbf{K}}_{(s)}^{IB} & \bar{\mathbf{K}}_{(s)}^{II} \end{bmatrix} \begin{bmatrix} \mathbf{q}_{(s)}^B \\ \mathbf{q}_{(s)}^I \end{bmatrix} = \begin{bmatrix} \mathbf{g}_{(s)}^B \\ \mathbf{g}_{(s)}^I \end{bmatrix} + \begin{bmatrix} \mathbf{p}_{(s)}^B \\ \mathbf{0} \end{bmatrix}$$

and apply Hurty-Craig-Bampton:

$$\mathbf{q}_{(s)} = \begin{bmatrix} \mathbf{q}_{(s)}^B \\ \mathbf{q}_{(s)}^I \end{bmatrix} = \begin{bmatrix} \mathbf{I}_{(s)}^{BB} & \mathbf{0} \\ \boldsymbol{\Psi}_{(s)}^{IB} & \boldsymbol{\Phi}_{(s)}^{II} \end{bmatrix} \begin{bmatrix} \mathbf{q}_{(s)}^B \\ \boldsymbol{\eta}_{(s)}^I \end{bmatrix} \triangleq \mathbf{X}_{(s)} \boldsymbol{\gamma}_{(s)}$$

Short Course on Experimental Dynamic Substructuring, © 2020

15

Theory

After primal assembly, the linearized system looks like

$$\begin{bmatrix} \tilde{\mathbf{M}}_{CB}^{BB} & \tilde{\mathbf{M}}_{CB}^{BI} \\ \tilde{\mathbf{M}}_{CB}^{IB} & \mathbf{I}_{CB}^{II} \end{bmatrix} \begin{bmatrix} \ddot{\mathbf{q}}_{CB}^B \\ \ddot{\boldsymbol{\eta}}_{CB}^I \end{bmatrix} + \begin{bmatrix} \tilde{\mathbf{K}}_{CB}^{BB} & \mathbf{0} \\ \mathbf{0} & \omega_{CB}^2 \end{bmatrix} \begin{bmatrix} \mathbf{q}_{CB}^B \\ \boldsymbol{\eta}_{CB}^I \end{bmatrix} = \begin{bmatrix} \tilde{\mathbf{g}}_{CB}^B \\ \tilde{\mathbf{g}}_{CB}^I \end{bmatrix}$$

If many components are present and/or the interface is large, the ROM is still large. We can then apply *interface reduction*

$$\tilde{\mathbf{M}}_{CB}^{BB} \ddot{\mathbf{q}}_{CB}^B + \tilde{\mathbf{K}}_{CB}^{BB} \mathbf{q}_{CB}^B = \tilde{\mathbf{g}}_{CB}^B$$

By extracting dominant modes on the interface dofs only (internal dynamics is statically condensed)

$$(\tilde{\mathbf{K}}_{CB}^{BB} - \tilde{\omega}_j^2 \tilde{\mathbf{M}}_{CB}^{BB}) \tilde{\boldsymbol{\phi}}_j^{BB} = \mathbf{0}, \quad j = 1, \dots, n_{CB}^B$$

Short Course on Experimental Dynamic Substructuring, © 2020

16

Theory

The interface is then reduced as:

$$\xi_{CB} = \begin{bmatrix} q_{CB}^B \\ \eta_{CB}^I \end{bmatrix} = \begin{bmatrix} \tilde{\Phi}^{BB} & 0 \\ 0 & I \end{bmatrix} \begin{bmatrix} \eta_{CC}^B \\ \eta_{CB}^I \end{bmatrix} \triangleq X_{CC} \xi_{CC}$$

For two substructures, the final reduction basis looks like

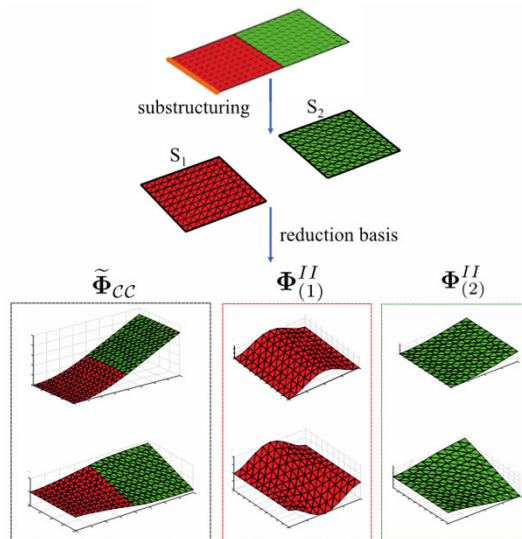
$$q_G = \begin{bmatrix} q_{(1)}^B \\ q_{(1)}^I \\ q_{(2)}^B \\ q_{(2)}^I \end{bmatrix} = \underbrace{\begin{bmatrix} I_{(1)}^{BB} & 0 & 0 & 0 \\ \Psi_{(1)}^{IB} & \Phi_{(1)}^{II} & 0 & 0 \\ 0 & 0 & I_{(2)}^{BB} & 0 \\ 0 & 0 & \Psi_{(2)}^{IB} & \Phi_{(2)}^{II} \end{bmatrix}}_{X_G} \underbrace{\begin{bmatrix} I_{(1)}^{BB} & 0 & 0 \\ 0 & I_{(1)}^{II} & 0 \\ I_{(2)}^{BB} & 0 & 0 \\ 0 & 0 & I_{(2)}^{II} \end{bmatrix}}_{L_{CB}} \underbrace{\begin{bmatrix} \tilde{\Phi}^{BB} & 0 & 0 \\ 0 & I_{(1)}^{II} & 0 \\ 0 & 0 & I_{(2)}^{II} \end{bmatrix}}_{X_{CC}} \begin{bmatrix} \eta_{CC}^B \\ \eta_{(1)}^I \\ \eta_{(2)}^I \end{bmatrix} =$$

$$\begin{bmatrix} \tilde{\Phi}_{(1)}^{BB} & 0 & 0 \\ \tilde{\Phi}_{(1)}^{IB} & \Phi_{(1)}^{II} & 0 \\ \tilde{\Phi}_{(2)}^{BB} & 0 & 0 \\ \tilde{\Phi}_{(2)}^{IB} & 0 & \Phi_{(1)}^{II} \end{bmatrix} \begin{bmatrix} \eta_{CC}^B \\ \eta_{(1)}^I \\ \eta_{(2)}^I \end{bmatrix}$$

Short Course on Experimental Dynamic Substructuring, © 2020

17

Linear HCB + Interface reduction



Short Course on Experimental Dynamic Substructuring, © 2020

18

Enhancement with modal derivatives

It is now possible to compute MDs for

- ✓ The internal VMs of each substructure

$$\theta_{jl,(s)}^{II} \triangleq \left. \frac{\partial^2 \mathbf{u}_{(s)}^I}{\partial y_{l,(s)} \partial y_{j,(s)}} \right|_0 = - \left(\bar{\mathbf{K}}_{(s)}^{II} \right)^{-1} \left. \frac{\partial \mathbf{K}_{(s)}^{II}}{\partial y_{l,(s)}} \right|_0 \phi_{j,(s)}^{II}$$

$$\left[\phi_{1,(s)}^{II} \quad \dots \quad \phi_{m_{I(s)},(s)}^{II} \quad \dots \quad \theta_{jl,(s)}^{II} \quad \dots \right] \triangleq \left[\Phi_{(s)}^{II} \quad \Theta_{(s)}^{II} \right]$$

- ✓ The Characteristic Constraint Modes (CCMs) (analogous formula)

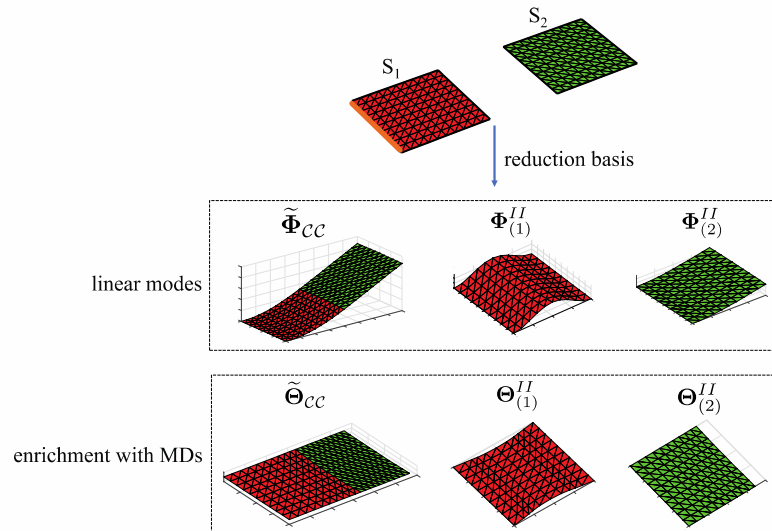
The internal and interface reduction is now enriched with MDs

$$\mathbf{u}_{(s)}^I = \begin{bmatrix} \Phi_{(s)}^{II} & \Theta_{(s)}^{II} \end{bmatrix} \begin{bmatrix} \eta_{(s)}^I \\ \zeta_{(s)}^I \end{bmatrix} \quad \mathbf{u}_G = \begin{bmatrix} \tilde{\Phi}_{CC} & \tilde{\Theta}_{CC} \end{bmatrix} \begin{bmatrix} \eta_{CC}^B \\ \zeta_{CC}^B \end{bmatrix}$$

Short Course on Experimental Dynamic Substructuring, © 2020

19

Enhancement with modal derivatives



Short Course on Experimental Dynamic Substructuring, © 2020

20

Reduced forces

Due to the polynomial form of von-Karman kinematics, the internal forces can be expressed directly in modal coordinates

$$\tilde{\mathbf{f}}_{(s)} = {}^2\tilde{\mathbf{Q}}_{(s)}\xi_{(s)} + \left({}^3\tilde{\mathbf{Q}}_{(s)} \cdot \xi_{(s)}\right)\xi_{(s)} + \left[\left({}^4\tilde{\mathbf{Q}}_{(s)} \cdot \xi_{(s)}\right) \cdot \xi_{(s)}\right]\xi_{(s)}$$

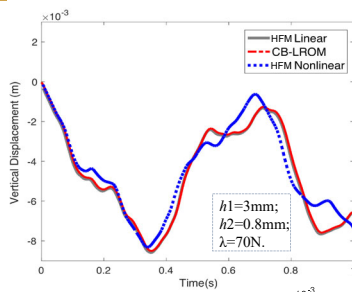
Computed offline once modes are known

The tangent stiffness matrix is likewise obtained.

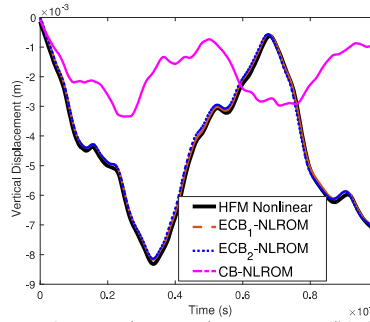
Short Course on Experimental Dynamic Substructuring, © 2020

21

Thick-thin plate

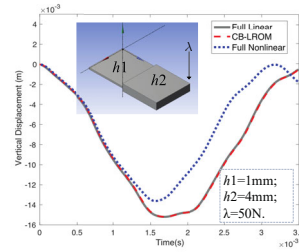


Reduction Basis	S_1	S_2	B	
CB-LROM	number of IVMs	number of SCC modes	total DoFs	
	5	10	10	25
ECB ₁ -NLROM	number of IVMs	number of SCC modes	total DoFs	
	5	10	10	
	number of MDs	number of MDs	10	65
ECB ₂ -NLROM	number of IVMs	number of SCC modes	total DoFs	
	5	10	10	
	number of MDs	number of MDs	0	45
CB-NLROM	number of IVMs	number of SCC modes	total DoFs	
	120	120	66	306

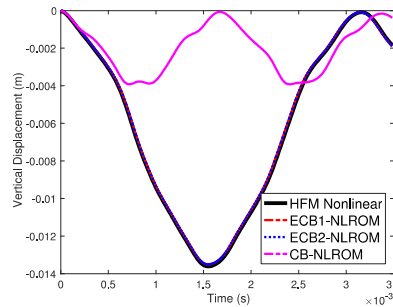


22

Thin-thick plate



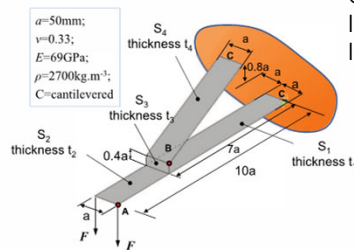
Reduction Basis	S_1	S_2	B	
CB-LROM	number of IVMs	number of SCC modes	total DoFs	
	10	5	10	25
ECB1-NLROM	number of IVMs	number of SCC modes	total DoFs	
	10	5	10	
	number of MDs	number of MDs	15	66
ECB2-NLROM	number of IVMs	number of SCC modes	total DoFs	
	10	5	10	
	number of MDs	number of MDs	15	60
CB-NLROM	number of IVMs	number of SCC modes	total DoFs	
	120	120	66	306



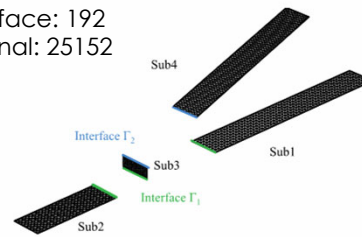
Short Course on Experimental Dynamic Substructuring, © 2020

23

Joined Wing



dof: 25344
Interface: 192
Internal: 25152



Sketch of the joined wing model

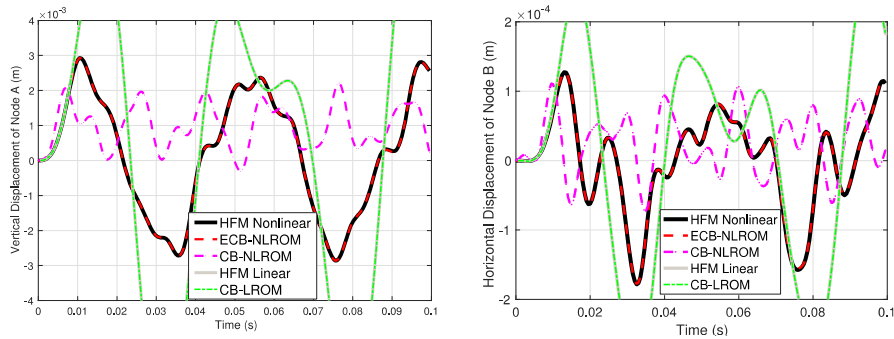
FE model of substructures

Methods	S_1	S_2	S_3	S_4	B	
CB-LROM	number of IVMs	number of SCC modes	total DoFs			
	10	10	10	10	10	50
ECB-NLROM	number of IVMs	number of SCC modes	total DoFs			
	10	10	10	10	10	
	number of MDs	number of MDs	15	15	15	125
CB-NLROM	number of IVMs	number of CMs	total DoFs			
	50	50	50	50	192	392

Short Course on Experimental Dynamic Substructuring, © 2020

24

Joined Wing



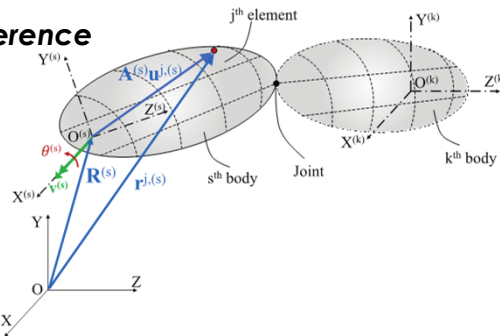
Numerical models	CPU time		speed up factor S_u	Global relative error $GRE_m(\%)$
	$t_{full}(s)$	$t_{red}(s)$		
Model-I(1)	65.36	5.78	11.31	1.52
Model-I(2)	70.59	7.23	9.76	1.31
Model-II	1194	16.65	71.71	0.54

Short Course on Experimental Dynamic Substructuring, © 2020

25

Flexible Multibody Systems

Floating frame of reference



$$\mathbf{r}^{j,(s)} = \mathbf{R}^{(s)} + \mathbf{A}^{(s)} \mathbf{u}^{j,(s)} = \mathbf{R}^{(s)} + \mathbf{A}^{(s)} \mathbf{N}^{j,(s)} \left(\mathbf{q}_0^{j,(s)} + \mathbf{q}_f^{j,(s)} \right)$$

- ✓ Each component referred to its own frame
- ✓ Allows for substructuring and independent reduction
- ✓ Rigid and flexible joints possible

Short Course on Experimental Dynamic Substructuring, © 2020

26

Multibody EoMs

$$\begin{aligned}
 &\text{Configuration-dependent mass matrix} \\
 &\begin{bmatrix} M_{RR}^{(s)} & M_{R\theta}^{(s)} & M_{Rm}^{(s)} \\ M_{\theta R}^{(s)} & M_{\theta\theta}^{(s)} & M_{\theta m}^{(s)} \\ \text{sym} & & M_{mm}^{(s)} \end{bmatrix} \begin{bmatrix} \ddot{\mathbf{R}}^{(s)} \\ \ddot{\boldsymbol{\theta}}^{(s)} \\ \ddot{\mathbf{q}}_m^{(s)} \end{bmatrix} - \begin{bmatrix} \mathbf{Q}_R^{(s)} \\ \mathbf{Q}_\theta^{(s)} \\ \mathbf{Q}_m^{(s)} \end{bmatrix} + \begin{bmatrix} \mathbf{0} \\ \mathbf{0} \\ \mathbf{f}_m^{(s)} \end{bmatrix} + \begin{bmatrix} (\mathbf{C}_R^{(s)})^T \\ (\mathbf{C}_\theta^{(s)})^T \\ (\mathbf{C}_m^{(s)})^T \end{bmatrix} \boldsymbol{\lambda} = \begin{bmatrix} \mathbf{g}_R^{(s)} \\ \mathbf{g}_\theta^{(s)} \\ \mathbf{g}_m^{(s)} \end{bmatrix} \\
 &\text{Constraints: } \mathbf{C}[\mathbf{R}, \boldsymbol{\theta}, \mathbf{q}_{m,v}] = \mathbf{0} \\
 &\text{Labels: Floating frame dofs, Elastic dofs, Inertial forces, Nonlinear elastic forces, Constraint forces, Gen. ext. load}
 \end{aligned}$$

Achieve reduction by **Component Mode Synthesis**

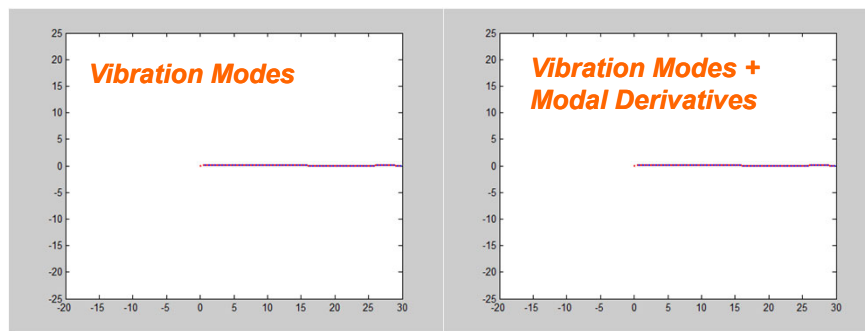
Short Course on Experimental Dynamic Substructuring, © 2020

27

Flexible Multibody Systems



Dr. Long Wu



L. Wu, P. Tiso, *Nonlinear model order reduction for flexible multibody dynamics: a modal derivatives approach*, Multibody System Dynamics, 2016

- ✓ Hurty-Craig-Bampton reduction per component
- ✓ nodal fixed frame
- ✓ Single node interface

Paolo Tiso

Short Course on Experimental Dynamic Substructuring, © 2020

28

Floating Frame Definition

Accuracy of approximate kinematics models (i.e. von Karman) improves if *relative displacements are minimized*

Mean Axis: dynamically define the FFR position and orientation by minimizing the relative kinetic energy.

Relative kinetic energy:

$$\mathcal{T}_r = \sum_j \frac{1}{2} \int_{V^j} \rho^j \left[\dot{\mathbf{r}}^j - \dot{\mathbf{R}} - \mathbf{B}^j \dot{\boldsymbol{\theta}}^j \right]^T \left[\dot{\mathbf{r}}^j - \dot{\mathbf{R}} - \mathbf{B}^j \dot{\boldsymbol{\theta}}^j \right] dV^j$$

Minimize w.r.t. the frame position and orientation:

$$\frac{\partial \mathcal{T}_r}{\partial \dot{\mathbf{R}}} = \mathbf{0} \quad \frac{\partial \mathcal{T}_r}{\partial \dot{\boldsymbol{\theta}}} = \mathbf{0} \quad \boldsymbol{\omega} = 2\mathbf{E}\dot{\boldsymbol{\theta}}$$

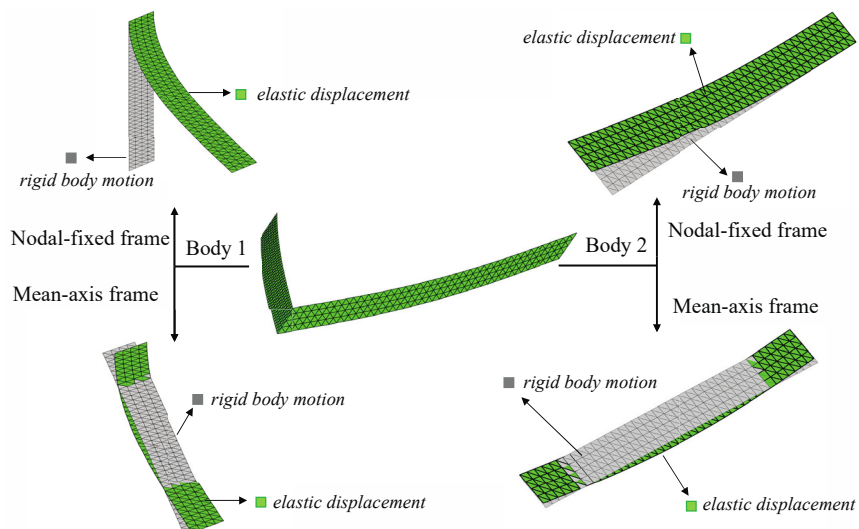
Linearize the constraint and integrate in time

$$\mathbf{S}\dot{\mathbf{q}}_f = \mathbf{0} \rightarrow \mathbf{S}\mathbf{q}_f = \mathbf{0}$$

Short Course on Experimental Dynamic Substructuring, © 2020

29

Nodal Fixed vs Mean Axis

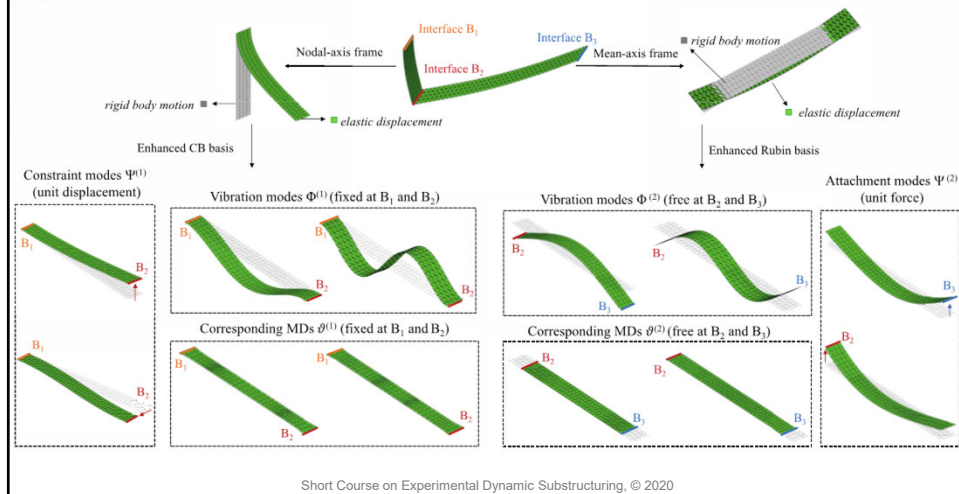


Short Course on Experimental Dynamic Substructuring, © 2020

30

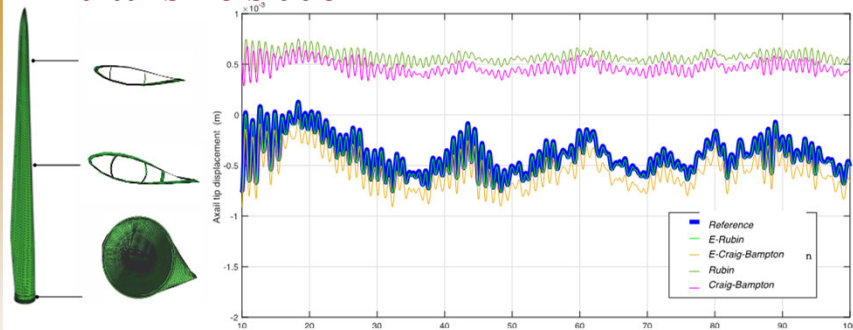
Component reduction basis

■ Use of the Rubin Method + modal derivatives



31

Wind turbine blade



floating frame	HFM	ROM		Number of iterations	speed up factor	
	t_{full}	offline	online	N	S_1	S_2
mean-axis	155307s	t_{off1}	t_{off2}	t_{on}		
nodal-fixed	49254s	13.25s	241s	125s	10598	129.87

Rubin + mean axis FFR outperforms Craig-Bampton + nodal fixed FFR

L.Wu, P. Tiso, K. A. van Keulen, K. Tatsis, E. Chatzi, **A modal derivatives enhanced Rubin substructuring method for geometrically nonlinear multibody systems**, Multibody System Dynamics, 2019

Short Course on Experimental Dynamic Substructuring, © 2020

32

Summary

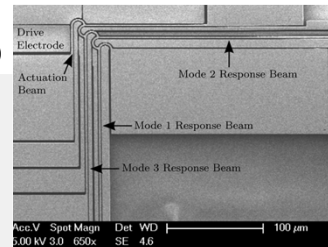
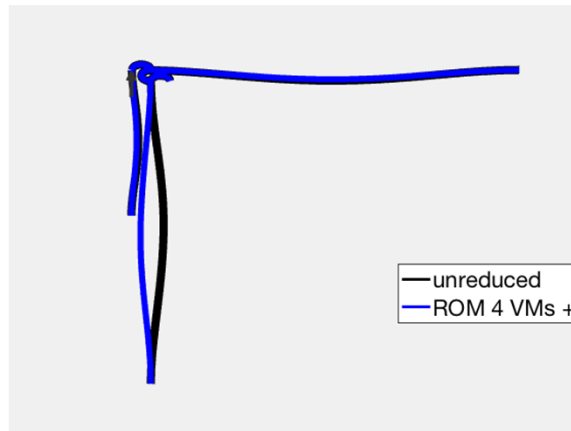
- **MDs can be applied in a substructuring context**, both on internal and interface modes
- They greatly improve the solution as compared to several high-frequency modes
- Role of MDs in reproducing **the rigid body modes** in highlighted
- In a floating frame of reference, the most promising combination seems mean axis definition + Rubin + MDs. This **minimizes the elastic deviation** from reference frame (and thus helps staying within the validity of the kinematic model) and **more naturally accounts for the rigid body motion**

Short Course on Experimental Dynamic Substructuring, © 2020

33

At this IMAC

Nonlinear substructuring for frequency dividers (parametric resonance)



A Component Mode Synthesis Method for the Nonlinear Dynamics Analysis of Frequency Dividers
#7602 | J. van der Broek–TU Delft; J. Marconi–Politecnico di Milano; P. Tiso–ETH Zürich; F. Aljani–Delft University of Technology

Short Course on Experimental Dynamic Substructuring, © 2020

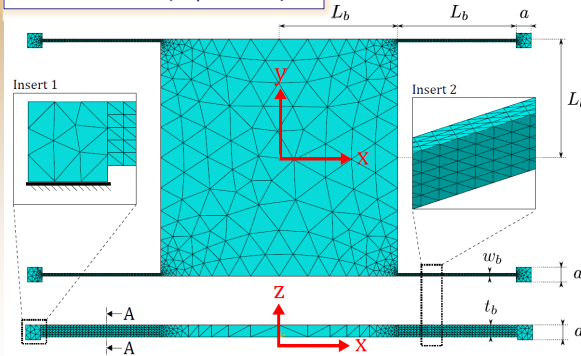
34

34

At this IMAC

Geometrically nonlinear ROM with embedded parametrized defects.

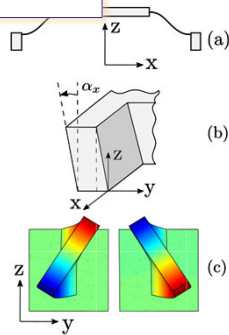
NOMINAL MESH (91,212 dofs)



(a) second VM, (b) wall angle, (c) twist of the beams

A Nonlinear Reduced Order Model with Parametrized Shape Defects #7613 | J. Marconi– Politecnico di Milano; P. Tiso–ETH Zürich; F. Braghin– Politecnico di Milano

3 DEFECTS



ACTUATION MODE (ϕ_1)

